Statistics of random lasing modes in weakly scattering systems

Xiaohua Wu and Hui Cao*

Department of Physics and Astronomy, Northwestern University, 2145 Sheridan Road, Evanston, Illinois, 60208, USA

**Corresponding author: h-cao@northwestern.edu*

Received August 1, 2007; revised August 28, 2007;
posted September 27, 2007 (Doc. ID 85870); published October 18, 2007

We investigated the statistics of random lasing modes in colloidal solutions with local pumping. The ensemble-averaged spectral correlation function of single-shot emission spectra exhibits regular oscillations. The statistical distribution of laser emission intensity follows a power-law decay, in comparison with an exponential decay of the statistical distribution of amplified spontaneous emission (ASE) intensity. The dramatic difference between the statistics of lasing peaks and that of the stochastic ASE spikes illustrates their distinct mechanisms. © 2007 Optical Society of America

OCIS codes: 290.4210, 140.3460.

A random laser is a nonconventional laser whose feedback is mediated by random fluctuations of the dielectric constant in space. The formation of resonant lasing modes relies on the interference of scattered waves that return to the same coherence volume via different closed paths. The coherent interference effect selects the lasing frequencies, leading to discrete narrow peaks in the lasing spectrum [1]. Because the modes vary from sample to sample, their lasing characteristic can only be described quantitatively in terms of statistics. Despite many experimental studies on random lasers, there have been few related to the statistics of lasing modes [2,3]. In addition to the lasing peaks, stochastic spikes are observed in the single-shot spectra of amplified spontaneous emission (ASE) from colloidal solutions over a wide range of scattering strength [4]. They are attributed to single spontaneous emission events that happen to take long open paths inside the amplifying random medium and pick up a large gain. It is not known how the statistics of random lasing peaks differ from that of the ASE spikes. In this Letter, we present a systematic experimental study on the statistical properties of random lasing modes and compare them with those of the ASE spikes. The spectral correlations and intensity statistics of lasing peaks are obtained with the colloidal solutions under local pumping. They are very different from those of the ASE spikes, underlying their distinct physical mechanisms.

Our experiments were performed on the diethylene glycol solutions of Stilbene 420 dye and TiO_2 particles (mean radius, 200 nm). The experimental setup was the same as that in [5]. The motion of particles in the solution provides different random configurations for each pump pulse, which facilitates the ensemble measurement under identical conditions. The Stilbene 420 was intentionally chosen for the weak reabsorption of emitted light outside the pumped region. The absorption length l_a at the center emission wavelength $\lambda_e = 427$ nm was 6 cm at the dye concentration $M = 8.5$ mM. It was much larger than the dimension (~1 cm) of the cuvette that holds the solution. At the particle density $\rho = 3 \times 10^9$ cm^{-3}, the scattering mean free path $l_s \simeq 1.3$ mm at the pump wavelength $\lambda_p = 355$ nm, and $l_s \simeq 1.0$ mm at λ_e. Although $l_a \simeq 10$ μm at λ_p, the pump light penetrated much deeper than l_a due to the saturation of absorption by intense pumping. The excitation volume had a cone shape with a length of a few hundred micrometers and a base diameter of 30 μm. Because its length was smaller than l_s, the excitation cone is almost identical to that of the neat dye solution. For the emitted light, the transport was diffusive in the entire colloidal solution whose dimension is much larger than l_s. Light amplification, however, occurred only in the pumped region having a size of the sub-mean free path.

The single-shot emission spectra from the colloidal solution are shown in Figs. 1(a)–1(c) with increasing pump pulse energy E_p. At $E_p = 0.05$ μJ [Fig. 1(a)], the spectrum exhibits sharp spikes on top of a broad ASE band. From shot to shot the spikes change com-

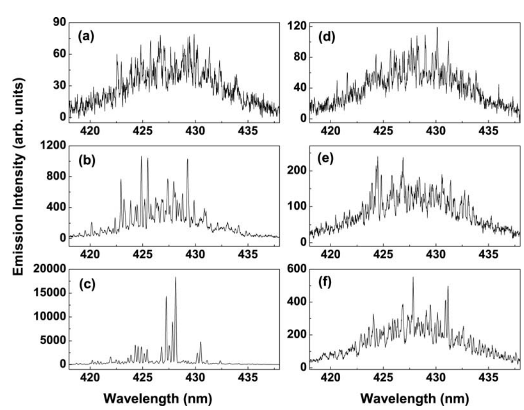

Fig. 1. Single-shot spectra of emission from the 8.5 mM Stilbene 420 dye solutions (a)–(c) with and (d)–(f) without TiO_2 particles. The particle density $\rho = 3 \times 10^9$ cm^{-3} in (a)–(c). The pump pulse energy $E_p = 0.05$ μJ for (a) and (d), 0.09 μJ for (b) and (e), 0.13 μJ for (c) and (f).

pletely. The typical linewidth of the spikes is ~ 0.07 nm. The neighboring spikes often overlap partially. As pumping increases, the spikes grow in intensity. When E_p exceeds a threshold, a different type of peak emerges in the emission spectrum [Fig. 1(b)]. These peaks grow much faster with pumping than the spikes and dominate the emission spectrum at $E_p = 0.13\ \mu$J [Fig. 1(c)]. These peaks, with a typical width of 0.13 nm, are notably broader than the spikes. Unlike the spikes, the spectral spacing of adjacent peaks is more or less regular. We have repeated the experiment with solutions of different ρ as well as the neat dye solution of the same M. The peaks can only be observed with particles in the solution, while the spikes appear also in the spectrum of emission from the neat dye solution [Figs. 1(d)–1(f)]. Although they are similar at $E_p = 0.05\ \mu$J, the emission spectra with and without particles are dramatically different at $E_p = 0.13\ \mu$J. Even under intense pumping, the emission spectrum of the neat dye solution has only spikes but no peaks [Fig. 1(f)]. The maximum spike intensity is ~ 50 times lower than the maximum peak intensity from the colloidal solution at the same pumping [Fig. 1(c)]. While the pump threshold for the appearance of peaks depends on ρ, the threshold for the emergence of spikes in solutions with low ρ is similar to that with $\rho = 0$.

In our previous experimental and numerical studies [5], we concluded that the large peaks represent the lasing modes formed by the distributed feedback in the colloidal solution. Although the feedback is weak at low ρ, the intense pumping strongly amplifies the backscattered light and greatly enhances the feedback. In contrast, the feedback from the particles is not necessary for the spikes that also exist in the neat dye solution. Thus the spikes are attributed to the ASE.

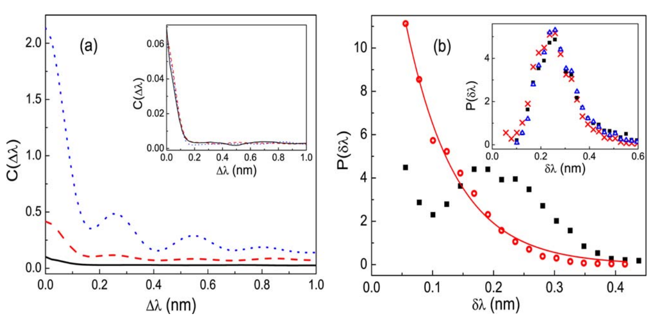

Fig. 2. (Color online) (a) Ensemble-averaged spectral correlation function $C(\Delta\lambda)$ of single-shot emission spectra. $M = 8.5$ mM. $\rho = 3\times 10^9\ \mathrm{cm}^{-3}$ in the main panel, and 0 in the inset. $E_p = 0.05\ \mu$J (solid curves), $0.09\ \mu$J (dashed curves) and $0.13\ \mu$J (dotted curves). (b) Statistical distribution $P(\delta\lambda)$ of wavelength spacing $\delta\lambda$ between adjacent spikes or peaks selected by the three-point peak-finding method. $\rho = 0$ (circles), $3\times 10^9\ \mathrm{cm}^{-3}$ (squares). $E_p = 0.13\ \mu$J. The solid curve is an exponential fit $P(\delta\lambda) = 22\exp(-\delta\lambda/0.082)$. Inset, $P(\delta\lambda/\langle\delta\lambda\rangle)$ for $\rho = 3\times 10^9\ \mathrm{cm}^{-3}$ and $E_p = 0.13\ \mu$J, obtained with three methods: five-point peak-finding (squares), three-adjacent-point averaging followed by three-point peak-finding (crosses), or five-point peak-finding (triangles).

We investigated the spectral correlations and intensity statistics of lasing peaks and ASE spikes. The ensemble-averaged spectral correlation function $C(\Delta\lambda)$ is obtained from 200 single-shot emission spectra acquired under identical conditions. We chose the wavelength range 425–431 nm, within which the gain coefficient had only a small variation, to compute $C(\Delta\lambda) = \langle I(\lambda)I(\lambda+\Delta\lambda)\rangle / \langle I(\lambda)\rangle\langle I(\lambda+\Delta\lambda)\rangle - 1$. For $\rho = 3\times 10^9\ \mathrm{cm}^{-3}$, $C(\Delta\lambda)$ changed dramatically with pumping [Fig. 2(a)]. Below the lasing threshold, it started with a small value at $\Delta\lambda = 0$ and decayed quickly to zero as $\Delta\lambda$ increased. Above the lasing threshold, the amplitude of $C(\Delta\lambda)$ grew rapidly, and regular oscillations with $\Delta\lambda$ developed. The oscillation period is ~ 0.27 nm, corresponding to the average spacing of lasing peaks. Despite the lasing peaks, change from shot to shot, the oscillations survived the ensemble average. This result confirms that the lasing peaks in a single-shot spectrum were more or less regularly spaced and that the average peak spacing was nearly the same for different shots. In contrast, $C(\Delta\lambda)$ for the ASE spikes at $\rho = 0$ barely changed with pumping [inset of Fig. 2(a)]. It is similar to that of the colloidal solution below the lasing threshold where the spectrum has only ASE spikes. Although the ASE spikes produce irregular oscillations in the spectral correlation function of an individual single-shot spectrum, such oscillations are smeared out after averaging over many shots. This result reflects the stochastic nature of the ASE spikes.

We obtained the statistical distribution $P(\delta\lambda)$ of wavelength spacing $\delta\lambda$ between adjacent lasing peaks and ASE spikes. The spectral resolution of our spectrometer is limited by the pixel size of the CCD array detector. Each pixel corresponds to a wavelength interval $d\lambda = 0.02$ nm. An ASE spike typically covers $3-4 d\lambda$; a lasing peak, $7-8 d\lambda$. We use the three-point peak-finding method, $I(\lambda) > I(\lambda \pm d\lambda)$, to identify a spike or peak at λ. Figure 2(b) presents $P(\delta\lambda)$ for $\rho = 0$, $3\times 10^9\ \mathrm{cm}^{-3}$, and $E_p = 0.13\ \mu$J. Due to the finite width of spikes and peaks, we could not get $P(\delta\lambda)$ at $\delta\lambda$ near 0. Since the emission spectra of neat dye solution at high pumping have no lasing peaks and the ASE spikes dominate the background noise, $P(\delta\lambda)$ for $\rho = 0$ reflects the wavelength spacing of ASE spikes. The solid curve in Fig. 2(b) represents an exponential fit, $P(\delta\lambda) \sim \exp(-\delta\lambda/\langle\delta\lambda\rangle)$, where $\langle\delta\lambda\rangle = 0.08$ nm is the average spacing. It suggests that the spectral spacing of ASE spikes satisfies Poisson statistics, which means that the frequencies of individual ASE spikes are uncorrelated. $P(\delta\lambda)$ for $\rho = 3\times 10^9\ \mathrm{cm}^{-3}$ features a second maximum at $\delta\lambda \sim 0.2$ nm, which results from the lasing peaks. The first maximum at $\delta\lambda \sim 0$ corresponds to the ASE spikes, as both lasing peaks and ASE spikes are selected by the three-point peak-finding method. To exclude the ASE spikes, we used the five-point peak-finding method, i.e., $I(\lambda) > I(\lambda \pm d\lambda) > I(\lambda \pm 2d\lambda)$ to identify a peak at λ. Since the ASE spikes were narrow and closely packed, most of them were not selected. Consequently, $P(\delta\lambda)$ at $\delta\lambda$ close to 0 is greatly reduced [inset of Fig. 2(b)]. The local maximum at $\delta\lambda \sim 0.2$ nm was narrowed and shifted to larger $\delta\lambda$. It becomes the global maximum. To confirm this result, we tried a different method. The emission spectrum was first smoothed by three-adjacent-point averaging. Most ASE spikes are smeared out, while the lasing peaks remain. Then we used either the three-point peak-finding method or the five-point peak-finding method to identify the peaks. As shown in the inset of Fig. 2(b), $P(\delta\lambda)$ obtained with these methods were nearly identical. They all reach the maximum at $\delta\lambda = 0.27$ nm, which coincides with the average lasing peak spacing obtained from the oscillation period of $C(\Delta\lambda)$. This result reflects the spectral repulsion of lasing modes.

To study the statistics of emission intensity, we first computed the average intensity $\langle I(\lambda)\rangle$ from 200 single-shot emission spectra, then extracted the statistical distribution of the normalized emission intensity $I(\lambda)/\langle I(\lambda)\rangle$ within the wavelength range 425–431 nm. In Fig. 3(a), the log–log plot of $P(I/\langle I\rangle)$ for $\rho = 3\times 10^9\ \mathrm{cm}^{-3}$ clearly reveals the power-law decay at large I above the lasing threshold. Solid lines represent the fitting $P(I/\langle I\rangle) \sim (I/\langle I\rangle)^{-b}$, with $b=3.3$, 2.5 for $E_p = 0.09\ \mu$J, 0.13 μJ. Since only the high lasing peaks contribute to the tail of $P(I/\langle I\rangle)$, the power-law decay reflects the intensity statistics of lasing peaks. Below the lasing threshold, $P(I/\langle I\rangle)$ is similar to that of the neat dye solution, which exhibits an exponential tail. As shown in the log-linear plot of Fig. 3(b), the exponential decay rate is almost the same for different pumping levels. The solid line is an exponential fit $P(I/\langle I\rangle) \sim \exp(-aI/\langle I\rangle)$ with $a=5.1$. In the absence of lasing peaks, the ASE spikes contribute to $P(I/\langle I\rangle)$ at large I. Therefore the exponential decay describes the intensity statistics of ASE spikes.

These experimental results demonstrate the fundamental difference between the ASE spikes and lasing peaks. The stochastic structures of the pulsed ASE spectra of neat dye solutions were observed long ago [6]. In our experiment, the observed ASE spikes originate from the photons spontaneously emitted near the excitation cone tip in the direction toward the cone base. As they propagated along the cone, these photons experienced the largest amplification due to their longest path length inside the gain volume. The ASE at the frequencies of these photons is the strongest, leading to the spikes in the emission spectrum. Since different ASE spikes originate from independent spontaneous emission events, their frequencies are uncorrelated, which leads to Poisson statistics of the frequency spacing of neighboring ASE spikes. In the colloidal solution of low ρ, the large aspect ratio of the excitation cone results in lasing along the cone, confirmed by the directionality of lasing output. The large gain inside the cone greatly amplified the feedback from the scatterers within the cone as compared with those from outside the cone. Thus the lasing modes deviate from the quasi-modes of the passive system, as demonstrated by our recent numerical simulation [7]. The statistical distribution of the decay rate of the quasi-modes cannot be applied directly to the calculation of $P(I/\langle I\rangle)$ [8–10]. Moreover, the mode competition and gain saturation, as well as the initial spontaneous emission into individual modes, must be taken into account to reproduce $P(I/\langle I\rangle)$. The rapid variation of gain in time and space make the calculation of intensity statistics even more difficult. We hope our data will stimulate further theoretical studies.

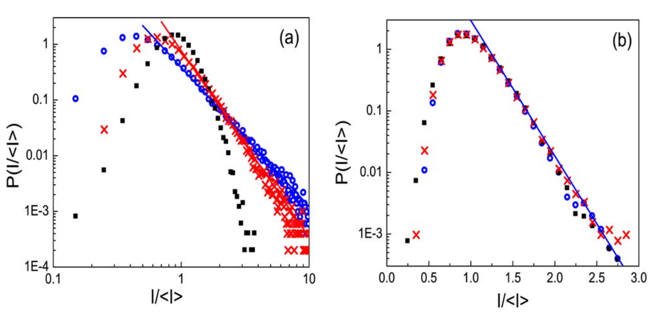

Fig. 3. (Color online) Statistical distributions of normalized emission intensities $I(\lambda)/\langle I(\lambda)\rangle$ for $425\ \mathrm{nm} < \lambda < 431\ \mathrm{nm}$. $\rho = 3\times 10^9\ \mathrm{cm}^{-3}$ in (a), and 0 in (b). $E_p = 0.05\ \mu$J (squares), 0.09 μJ (crosses), 0.13 μJ (circles). The solid lines represent curve fitting. In (a) $P(I/\langle I\rangle) = 0.77(I/\langle I\rangle)^{-3.3}$ (for crosses) and $P(I/\langle I\rangle) = 0.38(I/\langle I\rangle)^{-2.5}$ (for circles). In (b), $P(I/\langle I\rangle) = 467\exp(-5.1 I/\langle I\rangle)$.

The authors acknowledge A. Yamilov and A. Chabanov for stimulating discussions. This work is supported by the National Science Foundation under grants DMR-0093949 and ECS-0601249.

References

1. H. Cao, J. Phys. A **38**, 10497 (2005), and references therein.
2. X. Wu, A. Yamilov, H. Noh, H. Cao, E. W. Seelig, and R. P. H. Chang, J. Opt. Soc. Am. B **21**, 159 (2004).
3. K. L. van der Molen, R. W. Tjerkstra, A. P. Mosk, and A. Lagendijk, Phys. Rev. Lett. **98**, 143901 (2007).
4. S. Mujumdar, M. Ricci, R. Torre, and D. W. Wiersma, Phys. Rev. Lett. **93**, 053903 (2004).
5. X. Wu, W. Fang, A. Yamilov, A. A. Chabanov, A. A. Asatryan, L. C. Botten, and H. Cao, Phys. Rev. A **74**, 053812 (2006).
6. P. Sperber, W. Spangler, B. Meier, and A. Penzkofer, Opt. Quantum Electron. **20**, 395 (1988).
7. X. Wu, J. Andreasen, H. Cao, and A. Yamilov, J. Opt. Soc. Am. B **24**, A26 (2007).
8. M. Patra, Phys. Rev. E **67**, 016603 (2003).
9. V. M. Apalkov and M. E. Raikh, Phys. Rev. B **71**, 054203 (2005).
10. O. Zaitsev, Phys. Rev. A **74**, 063803 (2006).